Theoretical Analysis of Heteroaromatic Thioaminyl Radicals. Part 2: A Comparison of Ab Initio and Density Functional Methods in the Description of Redox Processes†

Piotr Kaszynski*

Organic Materials Research Group, Department of Chemistry, Vanderbilt University, Nashville, Tennessee 37235

Received: March 14, 2001; In Final Form: June 1, 2001

Gas-phase electron-transfer processes for 12 known thioaminyl radicals belonging to 7 general classes of heterocycles have been investigated using the HF and B3LYP methods with 6-31G(d) basis set augmented with diffuse functions. The basis set was chosen based on favorable comparison of the theoretical and experimental normal modes for **1a**. The calculated ionization potentials (I_p) and free energy changes were subsequently compared with the experimental I_p and electrochemical redox potentials. It was found that the DFT method performs better than the HF method giving excellent correlations for vertical I_p and $E^{red}_{1/2}$ ($R^2 > 0.98$), but not for $E^{ox}_{1/2}$ or E_{cell} ($R^2 = 0.7$). The calculated disproportionation energies were compared with the available conductivity data for radicals showing a qualitative correlation. Generally, low disproportionation energies and hence high conductivity are obtained for large π systems, such as **11**, containing the −N−S−S− array of heteroatoms. The established correlations provide a set of empirical scaling factors relating the calculated quantities with experimental observables for cyclic thioaminyl radicals. They were used in analysis of several radicals in the context of conductivity of molecular solids. A companion paper (ref 1) also appears in this issue [Kaszynski, P. *J. Phys. Chem. A* **2001**, *105,* 7615].

Introduction

Cyclic thioaminyl radicals have been studied intensively as molecular conductors.[2−7] Their electrically neutral open-shell π electronic architecture fits Haddon's model of a unidimensional conductor, which generally requires an infinite array of closely and regularly spaced neutral π radicals with low disproportionation and reorganization energies. While the first requirement is in the realm of crystal engineering, the second is a molecular design parameter and can be assessed from electrochemical studies.[8,9] Thus, the difference between solution oxidation and reduction potentials for a radical (cell electrochemical potential E_{cell}) is a measure of its disproportionation energy and represents the free energy change in the process. The disproportionation energy of neutral species into ion pairs largely determines the on-site Coulomb correlation energy,[10−12] and is a well established and important criterion for predicting conductivity of organic solids.[12]

Quantum mechanical methods can accurately calculate the electron affinity and ionization potentials,[13] which represent the gas-phase redox processes. Previous studies demonstrated a linear correlation between solution oxidation potentials ($E^{ox}_{1/2}$) and experimental gas-phase ionization potentials (I_p) for derivatives of **1a**,[9] and also satisfactory accuracy in computational estimation of I_p.[14−17] This suggests that the calculated I_p as well as electron affinity (EA) might be convenient tools for prediction of electrochemical behavior of new radicals and hence their donor−acceptor properties and disproportionation energies.

Our interest in liquid crystal radicals[18−21] prompted us to develop reliable computational protocols for predicting properties of new open-shell π-conjugated heterocycles suitable for construction of liquid crystalline materials, and hence rational design of new materials with desired bulk magnetic and electrical behavior. Among the key parameters in the design is the redox behavior of the mesogenic radicals. This affects intermolecular interactions in binary systems, and hence the structure and stability of the liquid crystal phase as well as electron transport phenomena in the material.

In the preceding paper,[1] we demonstrated that geometrical features of cyclic thioaminyl radicals are better reproduced by the HF method, but accurate computation of hfcc and spin density distribution in radicals **1**−**11** (Chart 1) require the electron correlation included in the DFT methods. In this paper we will continue our systematic comparison between the HF and B3LYP methods in an attempt to develop a computational protocol for predicting redox properties of new radicals. First, we verify the precision of the 6-31G(d) basis set, mainly used in the present studies, in reproducing normal modes. Second, we calculate ionization potentials and electron affinities and correlate them with solution oxidation and reduction potentials. Subsequently, disproportionation energies are calculated and compared with cell electrochemical potentials and the results of conductivity studies. Finally, we use the established correlations to assess molecular parameters for selected radicals.

Computational Methods

Quantum-mechanical calculations were carried out using the Gaussian 94[22] and Gaussian 98[23] (data in Table 5) packages on an SGI R8000 workstation using HF and B3LYP methods. All open-shell species were calculated using unrestricted methods. Following general recommendations,[24] electron affinities and disproportionation energies of radicals were derived as the differences of SCF energies of individual species computed

* Phone/fax: (615) 322-3458. Email: piotr@ctrvax.vanderbilt.edu.

† Presented, in part, at 215th ACS National Meeting, March 29−April 2, 1998, Dallas, TX, Abstr: COMP 145; and at the Structural and Mechanistic Organic Chemistry: A Tribute to Norman L. Allinger, Athens, GA, June 3−7, 1997.

10.1021/jp0109574 CCC: $20.00
Published on Web 07/24/2001

CHART 1

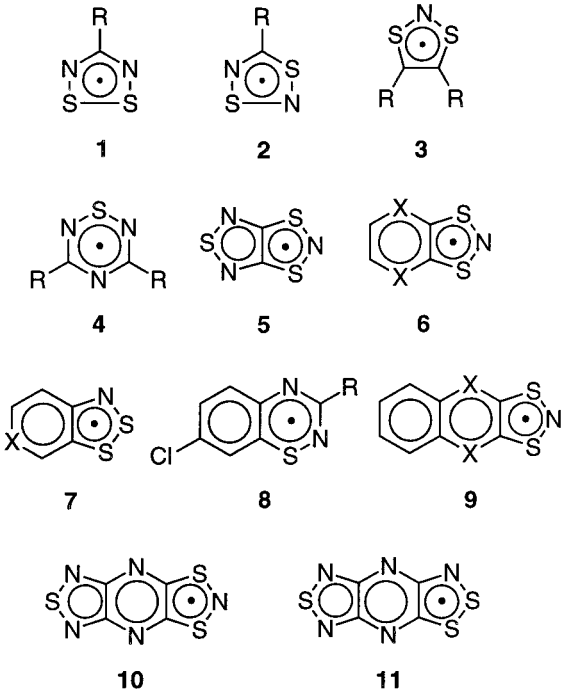

a R=H, **b**, R=F; **c**, R=Cl, **d**, R=CH_3; **e**, R=CF_3; **f**, R=CN; **g**, R=Ph **h**, X=CH; **i**, X=N

using the diffuse function-augmented 6-31+G(d) basis set at the geometries obtained with the 6-31G(d) basis set (single-point calculations). Thermodynamic corrections were obtained using the 6-31G(d) basis set. Other computational details are listed in the preceding paper,[1] and energies for the radicals and the ions derived from them are listed in Supporting Information.

Results and Discussion

A consideration of energetics of redox processes requires calculation of thermodynamic parameters. A good indicator of their quality is the agreement between experimental and theoretical vibrational frequencies. The recently reported gas-phase vibrational spectrum of **1a**[16] allows for assessment of HF/6-31G(d) and B3LYP/6-31G(d) methods in normal-mode calculation and hence thermodynamic corrections. Therefore, we first verify that the 6-31G(d) basis set is appropriate for further theoretical studies of radicals **1**−**11** by comparing the calculated and experimental normal modes for **1a**. Subsequent calculations are performed for radicals in their conformational ground states.[1]

Vibrational Spectrum for 1a. Normal modes for **1a** were calculated using the UB3LYP method with three basis sets and compared to the experimental data in Table 1 using the previous band assignment. Calculations at the UHF/6-31G(d) level of theory verify previous results[16] and agree with the relative positions of the B_2 and B_1 bands around 500 cm^{-1} and the A_1 and B_2 bands in the 700 cm^{-1} region. The UB3LYP calculations consistently show, however, that the assignment within the two sets of bands is reversed (Table 1).

In the experimental spectrum, vibrations in the region of 400−800 cm^{-1} overlap and the assignment is not completely clear. Switching the assignment of the bands at 729 and 757 reduces the STD from 18, 17, and 15 cm^{-1} to 11, 7, and 9 cm^{-1} for the vibrations obtained with 6-31G(d), 6-31G(2df), and cc-pVDZ basis sets, respectively. Exchanging positions for vibrations assigned to the 489 and 500 cm^{-1} bands has a negligible effect on the STD. Overall, the UB3LYP method reproduces the normal modes significantly better than the UHF method with the STD less than half of that for the UHF method for the 6-31G(d) basis set, and as low as 7 cm^{-1} for the 6-31G(2df) basis set.

The calculated wavenumbers of the normal modes were scaled by a factor defined in Table 1 and chosen in such a way that the mean difference between the calculated and experimental values is close to zero. The factors used for UHF/6-31G(d) and UB3LYP/6-31G(d) calculations are 4% and 1% larger, respectively, than the recommended values.[25]

Ionization Potentials and Electron Affinities. The literature ionization potentials (I_p) and electrochemical data for selected radicals are collected in Tables 2 and 3 and compared with results of HF and B3LYP calculations using the 6-31G(d) and 6-31+G(d) basis sets. The vertical I_p were obtained as ΔE_{SCF} for a single-point calculation of the corresponding cation at the radical geometry. The adiabatic I_p and electron affinity (EA) were obtained as ΔE_{SCF} of fully optimized ions and corrected for ZPE.

TABLE 1: Observed and Calculated Infrared Wavenumbers for 1a[a]

		calcd									
		UHF			UB3LYP						
obsd[b]		6-31G(d)				6-31G(d)		6-31G(2df)		cc-pVDZ	
freq	band type	sym	freq[c]	int.	sym	freq[d]	int	freq[e]	int	freq[f]	int
		A_2	225	0	A_2	262	0	258	0	236	0
		A_1	490	0.1	B_2	366	1.9	393	1.6	382	1.7
489	A	B_2	492	11	B_1*	491*	27	494*	23.8	495*	25.5
500	C	B_1	509	27	B_2*	497*	5	495*	6.6	497*	4.3
729	B	A_1	718	11	B_2#	722#	82	730#	70.5	725#	74.1
757	A	B_2	741	54	A_1#	746#	2.2	761#	5.1	748#	1.6
815	B	A_1	840	1.3	A_1	797	6.5	802	5.2	806	7.2
900	C	B_1	902	6.4	B_1	899	6.4	900	4.8	894	7.5
1196	A	B_2	1143	1.4	B_2	1212	9.4	1205	11.5	1215	10.1
1243	B	A_1	1244	33	A_1	1254	20.3	1250	23.3	1253	15.3
1333	A	B_2	1372	0.5	B_2	1342	0.9	1325	1.7	1331	2.0
		A_1	3180	5.7	A_1	3141	2.7	3088	1.8	3125	1.4
STD			27			11		7		9	

[a] Wavenumbers in cm^{-1} and theoretical intensities in km/mol. Symbols * and # define two pairs with interchanged band assignment. [b] Cordes, A. W.; Bryan, C. D.; Davis, W. M.; de Laat, R. H.; Glarum, S. H.; Goddard, J. D.; Haddon, R. C.; Hicks, R. G.; Kennepohl, D. K.; Oakley, R. T.; Scott, S. R.; Westwood, N. P. C. *J. Am. Chem. Soc.* **1993**, *115*, 7232. [c] Scaled by 0.9275. [d] Scaled by 0.9745. [e] Scaled by 0.9715. [f] Scaled by 0.9820.

TABLE 2: Experimental and Calculated Ionization Potentials (I_p) for Selected Radicals[a]

	calcd I_p [eV]								
	HF/6-31G(d)			B3LYP/6-31G(d)			exptl I_p [eV]		
	adiab.[c]	vert.	ΔG_{298}	adiab.[c]	vert.	ΔG_{298}	adiab.	vert.	$E^{ox}_{1/2}$[b] [V]
1a	7.967	8.333	8.058	7.825	7.991	7.886	7.87[d,e]	7.87[e]	0.65[f]
	8.026			7.859					
1c	8.231	8.618	8.321	8.004	8.215	8.066	7.73[g]	8.00[g]	0.83[f]
	8.290			8.038					
1e	8.357	8.742	8.425	8.135	8.331	8.185	7.94[g]	8.25[g]	0.91[f]
	8.412			8.164					
1g	7.830	8.260	7.973	7.264	7.451	7.326	7.10[g]	7.40[g]	0.60[h]
	7.945			7.297					
4c	8.438	9.063	8.536	8.395	8.756	8.441	8.18[g]	8.57[g]	*i*
	8.511			8.427					
4g	*j*	*j*	*j*	6.814	7.156	6.893	6.81[g]	7.35[g]	*i*
				6.853					
6h	6.688	7.098	6.770	6.564	6.743	6.646	6.3[k]	6.66[k]	0.15[k]
	6.736			6.612					
7h	7.064	7.371	7.206	6.665	6.786	6.742	*i*	*i*	0.26[l]0.18[m]
	7.168			6.713					
9h	6.683	7.081	6.758	6.459	6.616	6.535	*i*	*i*	0.27[n]
	6.724			6.503					
9i	7.166	7.625	7.232	6.941	7.093	7.003	*i*	*i*	0.62[n]
	7.200			6.975					
10	7.961	8.372	8.022	7.589	7.718	7.645	*i*	*i*	1.00[m,n]
	7.986			7.617					
11	8.741	9.257	8.891	7.794	7.888	7.847	*i*	*i*	1.14[m]
	8.848			7.820					

[a] Adiabatic I_p is the ΔE_{SCF} for fully optimized species and the vertical I_p is ΔE_{SCF} for species frozen at the radical geometry. [b] Measured in acetonitrile and referenced to SCE. Oxidation for all radicals is reversible. [c] Top values are calculated without ZPE correction, while the bottom numbers include ZPE. [d] Overlap with vertical I_p. [e] Cordes, A. W.; Bryan, C. D.; Davis, W. M.; de Laat, R. H.; Glarum, S. H.; Goddard, J. D.; Haddon, R. C.; Hicks, R. G.; Kennepohl, D. K.; Oakley, R. T.; Scott, S. R.; Westwood, N. P. C. *J. Am. Chem. Soc.* **1993**, *115*, 7232. [f] Boeré, R. T.; Moock, K. H. *J. Am. Chem. Soc.* **1995**, *117*, 4755. [g] Adiabatic I_p values assumed: Boeré, R. T.; Oakley, R. T.; Reed, R. W.; Westwood, N. P. C. *J. Am. Chem. Soc.* **1989**, *111*, 1180. [h] Boeré, R. T.; Moock, K. H.; Parvez, M. *Z. Anorg. Allg. Chem.* **1994**, *620*, 1589. [i] Not reported. [j] Not calculated. [k] Barclay, T. M.; Cordes, A. W.; de Laat, R. H.; Goddard, J. D.; Haddon, R. C.; Jeter, D. Y.; Mawhinney, R. C.; Oakley, R. T.; Palstra, T. T. M.; Patenaude, G. W.; Reed, R. W.; Westwood, N. P. C. *J. Am. Chem. Soc.* **1997**, *119*, 2633. [l] Tsveniashvili, V. Sh.; Malashluya, M. V. *Elektrokhim*. **1984**, *3*, 381. [m] Barclay, T. M.; Cordes, A. W.; Haddon, R. C.; Itkis, M. E.; Oakley, R. T.; Reed, R. W.; Zhang, H. *J. Am. Chem. Soc.* **1999**, *121*, 969. [n] Barclay, T. M.; Cordes, A. W.; George, N. A.; Haddon, R. C.; Itkis, M. E.; Mashuta, M. S.; Oakley, R. T.; Patenaude, G. W.; Reed, R. W.; Richardson, J. F.; Zhang, H. *J. Am. Chem. Soc.* **1998**, *120*, 352.

The plot in Figure 1 demonstrates that the ionization potentials calculated with either HF or B3LYP methods correlate well with the experimental values. Generally, the vertical I_p are reproduced better than the adiabatic I_p by either method, and the B3LYP method gives an overall better correlation with the experimental values in both cases. This is consistent with the previous findings that the inclusion of electron correlation significantly improves the calculated I_p values of dithiadiazolyl radicals **1**.[15] The intercept values in the best fit linear functions are statistically insignificant (smaller than 1σ) and set to 0.

Although a comparison of the calculated vertical ionization potentials with oxidation potentials ($E^{ox}_{1/2}$) measured in acetonitrile shows significant scattering, it demonstrates a clear trend (Figure 2). Compounds with high ionization potentials, such as monocyclic **1** and nitrogen-rich radicals, undergo oxidation at high potentials of about 1 V, while polycyclic hydrocarbon-based thioaminyl radicals are oxidized at low potentials of about 0.2 V. Surprisingly, the HF method performs somewhat better ($R^2 = 0.84$) than the DFT ($R^2 = 0.71$). Plots of the experimental $E^{ox}_{1/2}$ and the DFT-calculated adiabatic I_p or ΔG_{298} values also show poor correlation with slightly higher $R^2 = 0.74$.

A similar analysis of the data for the reduction of thioaminyl radicals shows excellent correlations between the calculated electron affinities (as ΔE_{SCF}) and reduction potentials ($E^{red}_{1/2}$) as shown in Figure 3. The plot contains data for fully reversible processes observed for **1a**[9] and **1g**,[9] **10**,[6,26] and **11**,[6] and also the cathodic peak potentials for irreversible reductions reported for other radicals. The B3LYP/6-31+G(d)//B3LYP/6-31G(d) calculated values correlate with the experimental data significantly better ($R^2 = 0.988$) than those obtained with the HF method ($R^2 = 0.86$), giving a best fit linear function with errors on the slope and intercept of about 4%. As observed for oxidation, there is little difference in correlation between solution reduction potentials and calculated EA as ΔE_{SCF}, corrected for ZPE or ΔG_{298}. This is fortunate since the correlation does not necessarily require expensive frequency calculations.

Large scattering in the correlation between ionization potentials and electrochemical data has been reported before and was attributed to reorganization energy and specific solvation.[27] The latter is particularly important in the case of cations in dipolar aprotic solvents, such as acetonitrile, in which the magnitude of interactions depends significantly on the charge distribution within the ion. In contrast, anions interact weakly with aprotic solvents and the electron transfer is expected to be less sensitive to solvation effects. This has indeed been observed experimentally for derivatives **1** and is consistent with our findings of a much better correlation between solution and gas-phase reduction than oxidation processes for several classes of compounds including **1a**. The reported $E^{ox}_{1/2}$ for **1** in acetonitrile are lower by 0.2 V relative to those measured in CH_2Cl_2, while the reduction potentials are virtually solvent independent.[9,28] Although the electrochemical results obtained in less polar solvents such as CH_2Cl_2 are preferred for comparison with gas-phase calculations, the majority of experimental data was obtained in acetonitrile, which is believed to mimic best the solid-state environment.

TABLE 3: Electron Affinity (EA) and Reduction Potential ($E^{red}_{1/2}$) for Selected Radicals[a]

	EA [eV]						
	HF/6-31+G(d)// HF/6-31G(d)			B3LYP/6-31+G(d)// B3LYP/6-31G(d)			
	ΔE_{SCF}	ΔE_0	ΔG_{298}	ΔE_{SCF}	ΔE_0	ΔG_{298}	$E^{red}_{1/2}$[b] [V]
1a	0.498	0.498	0.503	1.447	1.482	1.489	−0.83[c]
1c	1.014	1.011	1.004	1.882	1.916	1.941	−0.63[c]
1e	*d*	*d*	*d*	1.997	2.029	2.022	−0.42[c]
1g	0.343	0.283	0.280	1.542	1.583	1.586	−0.83[e]
6h	−0.186	−0.150	−0.156	0.996	1.046	1.043	−1.24[f,g]
7h	−0.113	−0.134	−0.153	1.356	1.406	1.404	−1.0[g]
9h	0.007	0.042	0.035	1.259	1.314	1.312	−1.08[h]
9i	0.396	0.424	0.423	1.734	1.786	1.802	−0.73[h]
10	1.029	1.054	1.072	2.504	2.530	2.527	−0.06[g,h]
11	1.397	1.321	1.313	2.911	2.932	2.933	0.15[g]

[a] ΔE_{SCF} and ΔE_0 are calculated as the difference of total energies between the radical and the geometry-optimized anion without and with ZPE, respectively. Thermodynamic corrections taken from calculations with the 6-31G(d) basis set. [b] Measured in acetonitrile and referenced to SCE. Reduction for all radicals except for **1a**, **1g**, **10**, and **11** is irreversible and reported as the cathodic peak potential. [c] Boeré, R. T.; Moock, K. H. *J. Am. Chem. Soc.* **1995**, *117*, 4755. [d] Not calculated. [e] Boeré, R. T.; Moock, K. H.; Parvez, M. *Z. Anorg. Allg. Chem.* **1994**, *620*, 1589. [f] Barclay, T. M.; Cordes, A. W.; de Laat, R. H.; Goddard, J. D.; Haddon, R. C.; Jeter, D. Y.; Mawhinney, R. C.; Oakley, R. T.; Palstra, T. T. M.; Patenaude, G. W.; Reed, R. W.; Westwood, N. P. C. *J. Am. Chem. Soc.* **1997**, *119*, 2633. [g] Barclay, T. M.; Cordes, A. W.; Haddon, R. C.; Itkis, M. E.; Oakley, R. T.; Reed, R. W.; Zhang, H. *J. Am. Chem. Soc.* **1999**, *121*, 969. [h] Barclay, T. M.; Cordes, A. W.; George, N. A.; Haddon, R. C.; Itkis, M. E.; Mashuta, M. S.; Oakley, R. T.; Patenaude, G. W.; Reed, R. W.; Richardson, J. F.; Zhang, H. *J. Am. Chem. Soc.* **1998**, *120*, 352.

The removal or addition of an electron to radicals has an impact on their geometry. As expected, oxidation of the radicals to the corresponding cations and the removal of an electron from the antibonding orbital generally causes shortening of bonding distances. For instance, the average change in the S−N bond length is −0.09 Å or −0.06 Å, according to the HF or B3LYP calculations, respectively. Normal-mode analysis of the cations confirmed their ground-state molecular symmetries and conformational preferences to be the same as those of the parent radicals. An exception is cation **1e**$^+$, which shows the staggered form as the conformational ground state according to the HF/6-31G(d) calculations.

Addition of an electron to the π^* orbital and formation of an anion is favorable for all radicals according to B3LYP/6-31+G(d)//B3LYP/6-31G(d) calculations, while the HF/6-31+G(d)//HF/6-31G(d) results show that for some species the reduction is endothermic (negative EA in Table 3). The reduction results in a lowering of the bond order and the elongation of ring bonds with an average change for the N−S distance of +0.06 Å or +0.07 Å, according to the HF or B3LYP calculations, respectively. The molecular symmetry is generally lowered and all heterocyclic rings except for **11**$^-$ undergo an out-of-plane distortion according to HF calculations. The B3LYP calculations generally agree with the HF results except for **1c**$^-$, **1g**$^-$, and **10**$^-$, in which the C_{2v} symmetry of the radical is retained in the anions. For example, the HF calculations predict a C_2 conformational minimum with a twist angle for the N−S−S−N group of 17.4° and 15.4° for **1c**$^-$ and **1g**$^-$, respectively.

Five-membered rings of fused heterocyclic anions adopt a puckered conformation in the ground state with the puckering angle decreasing from 46° in **6h**$^-$ through 40° in **9i**$^-$, 20° in **10**$^-$, and 0° in **11**$^-$, according to the HF calculations. The B3LYP results follow the same trend, but the change of the puckering angle in the series is faster: from 46° in **6h**$^-$ through 16° in **9i**$^-$ and 0° in **10**$^-$ and **11**$^-$ (Figure 4).

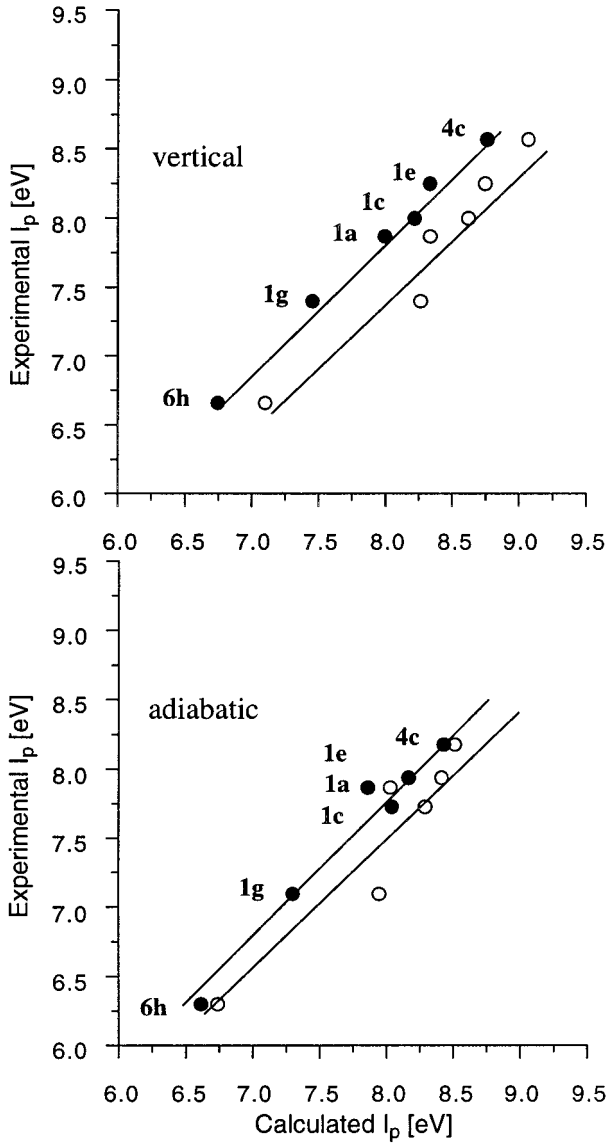

Figure 1. Plots of experimental vs theoretical vertical (a) and adiabatic (b) ionization potentials I_p (as ΔE_{SCF}) calculated using HF/6-31G(d) (open circles) and B3LYP/6-31G(d) (full circles) methods. The best fit functions for open circles: (a) $I_{p(exp)} = 0.933 \bullet I_{p(calcd)}$ ($R^2 = 0.944$) and (b) $I_{p(exp)} = 0.942 \bullet I_{p(calcd)}$ ($R^2 = 0.886$); for full circles: (a) $I_{p(exp)} = 0.984 \bullet I_{p(calcd)}$ ($R^2 = 0.993$) and (b) $I_{p(exp)} = 0.973 \bullet I_{p(calcd)}$ ($R^2 = 0.969$).

The distortion from planarity in the −N−S−S− isomers appears to be substantially smaller (by about 20°) than in the −S−N−S− compounds, as exemplified in the two pairs **6h**$^-$ and **7h**$^-$ and **10**$^-$ and **11**$^-$. B3LYP/6-31+G(d)//B3LYP/6-31G(d) calculations also show that while the free energy of planarization for the puckered **6h**$^-$ is substantial (8.3 kcal/mol), the puckered form of its isomer **7h**$^-$ represents only a shallow minimum on the potential energy surface (1.2 kcal/mol). This is presumably related to the larger degree of charge delocalization throughout the π system in the −N−S−S− isomer as shown for the two pairs in Figure 5.

Disproportionation Energies. Disproportionation of a neutral radical into a pair of closed-shell ions is a two-step process in which the initial electron transfer between a pair of radicals is followed by relaxation of the resulting Franck−Condon species. The energy of the first process defines the height of the barrier

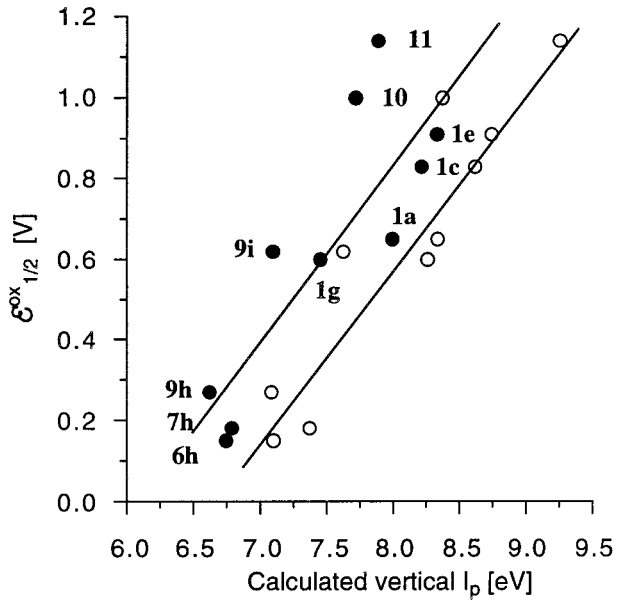

Figure 2. Plot of oxidation potential $E^{ox}_{1/2}$ in acetonitrile vs theoretical vertical ionization potential I_p calculated using HF/6-31G(d) (open circles) and B3LYP/6-31G(d) (full circles) methods. Best fit functions: $E^{ox}_{1/2} = 0.43 \bullet I_{p(calcd)} - 2.87$ ($R^2 = 0.87$, open circles) and $E^{ox}_{1/2} = 0.46 \bullet I_{p(calcd)} - 2.77$ ($R^2 = 0.71$, full circles).

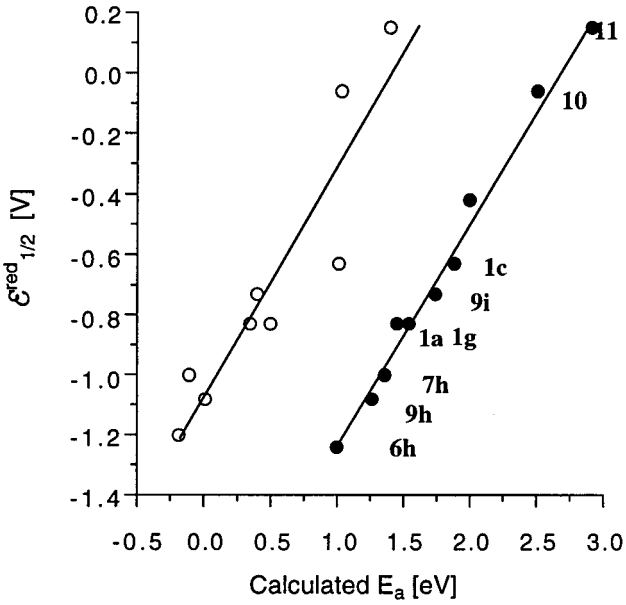

Figure 3. Plot of reduction potential $E^{red}_{1/2}$ in acetonitrile vs theoretical electron affinity EA (as ΔE_{SCF}) calculated using HF/6-31+G(d)//HF/6-31G(d) (open circles) and B3LYP/6-31+G(d)//B3LYP/6-31G(d) (full circles) methods. Best fit functions: $E^{red}_{1/2} = 0.76 \bullet EA - 1.06$ ($R^2 = 0.86$, open circles) and $E^{red}_{1/2} = 0.751 \bullet EA - 1.990$ ($R^2 = 0.988$, full circles).

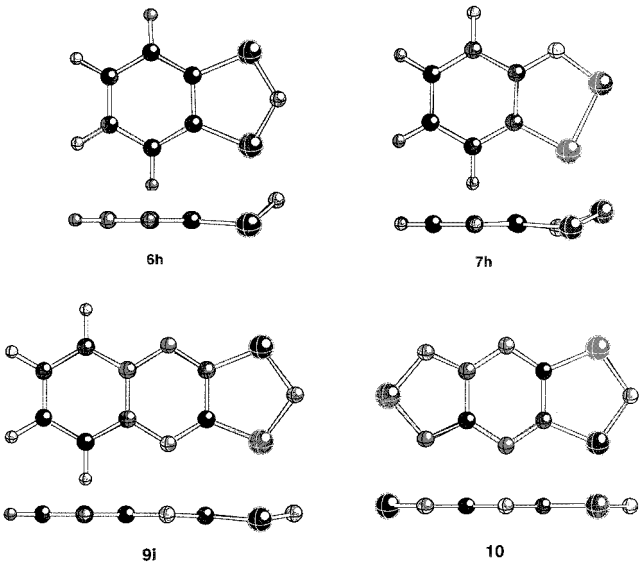

Figure 4. Equilibrium geometries for selected anions obtained with the B3LYP/6-31G(d) method.

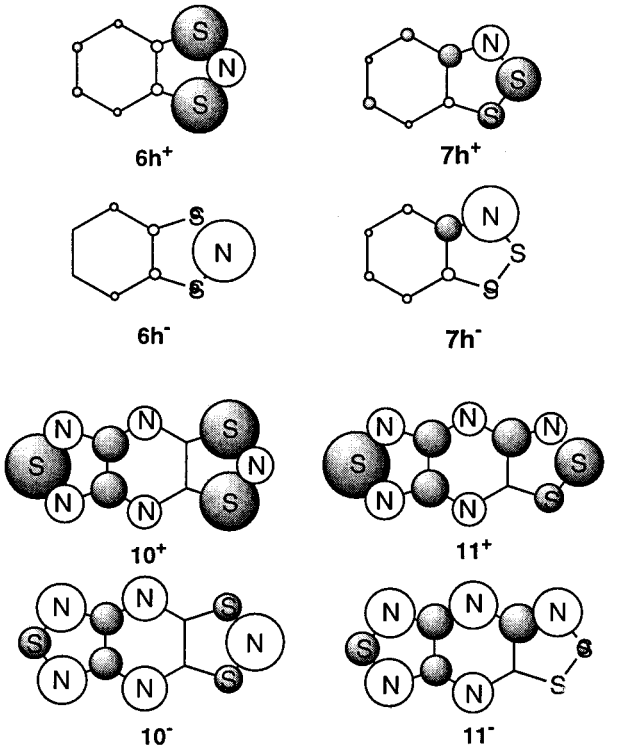

Figure 5. Mulliken atomic charge density maps for selected ions obtained with the B3LYP/6-31G(d) method. Hydrogen atomic charges are included in the charges of adjacent carbon atoms. Circles represent relative total positive (full circles) and negative (open circles) charge densities.

to disproportionation, while the relaxation energy describes the magnitude of the electron−phonon coupling and the tendency to undergo Peierls distortion in the solid state. For conducting materials, both energies are required to be small to minimize ionic fluctuations during current flow through the solid.

Although condensed-phase disproportionation energies depend significantly on the medium and specific ion solvation effects (vide supra), gas-phase calculations provide a reasonable and informative estimate of the relative magnitudes of these energies for a series of radicals and offer guidance for the design of molecular conductors. The measure of the medium effect on disproportionation energies can be assessed from the mathematical description of the correlation between the gas-phase calculation and solution electrochemical data in Figures 2, 3, and 6. Despite large scatter of the datapoints observed for oxidation processes, there is a clear trend, which should hold for the solid-state electron transfer. With this in mind, gas-phase redox processes for selected radicals were calculated and results collected in Table 4.

Data collected in Table 4 show that the electron-transfer energy ΔE^1_{SCF} is largest for small monocyclic radicals (158.0 kcal/mol for **1a**) and decreases as the size of the heterocycle increases (120.6 kcal/mol for **11**). This trend is consistent with the lower sensitivity of larger electronic systems to changes in

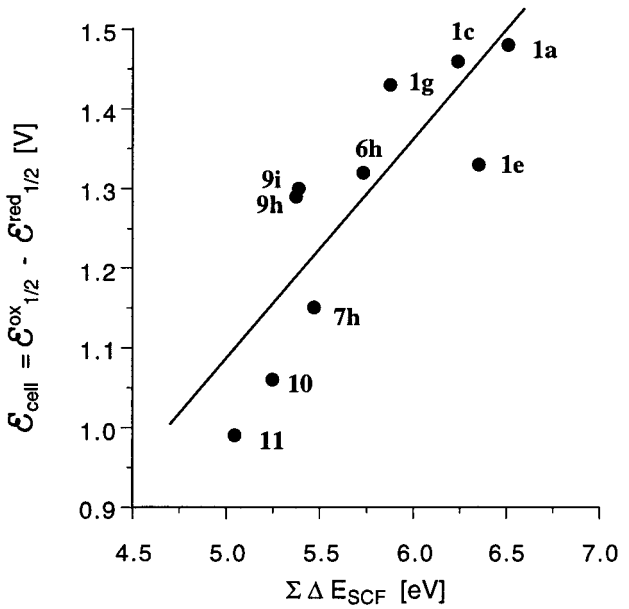

Figure 6. Plot of $E_{cell} = E^{ox}_{1/2} - E^{red}_{1/2}$ vs disproportionation energy $\Sigma\Delta E_{SCF} = E_{cat} + E_{an} - 2E_{rad}$ calculated using the B3LYP/6-31+G(d)//B3LYP/6-31G(d) method. Best fit function: $E_{cell} = 0.27 \bullet \Sigma\Delta E_{SCF} - 0.29$ ($R^2 = 0.69$).

TABLE 4: Calculated (B3LYP/6-31+G(d)//B3LYP/6-31G(d)) Disproportionation Energies for Selected Radicals[a]

$$2R\bullet \xrightarrow{\Delta E^1_{SCF}} [R^+ + R^-]^* \xrightarrow{\Delta E^2_{SCF}} R^+ + R^-$$

	ΔE^1_{SCF} [kcal/mol]	ΔE^2_{SCF} [kcal/mol]	$\Sigma\Delta E_{SCF}$ [kcal/mol]	$\Sigma\Delta G_{298}$ [eV]	E_{cell}[b] [V]
1a	158.0	−8.0	150.1	6.525	1.48[c]
1c	153.7	−9.8	143.9	6.241	(1.46)[c]
1e	155.7	−9.3	146.5	6.377	(1.33)[c]
1g	143.8	−8.3	135.5	5.892	1.43[c]
6h	147.3	−15.0	132.2	5.770	(1.32)[d]
7h	132.6	−6.5	126.1	5.496	(1.15)[e,f]
9h	133.8	−9.9	123.9	5.396	(1.29)[f,g]
9i	130.2	−6.1	124.2	5.378	(1.30)[f,g]
10	126.3	−5.3	121.0	5.279	1.06[g]
11	120.6	−4.3	116.3	5.073	0.99[e]
12[h]	116.5	−0.6	115.9	5.059	*i*

[a] ΔE^1_{SCF} is the electron-transfer energy and ΔE^2_{SCF} is the relaxation energy. $\Sigma\Delta E_{SCF}$ represent the energy of the overall process without ZPE. $\Sigma\Delta G_{298}$ is the overall change of free energy calculated at 298 K using thermodynamic corrections taken from calculations with the 6-31G(d) basis set. [b] $E_{cell} = E^{ox}_{1/2} - E^{red}_{1/2}$. Data for irreversible processes is in parentheses. [c] Boeré, R. T.; Moock, K. H. *J. Am. Chem. Soc.* **1995**, *117*, 4755. [d] Barclay, T. M.; Cordes, A. W.; de Laat, R. H.; Goddard, J. D.; Haddon, R. C.; Jeter, D. Y.; Mawhinney, R. C.; Oakley, R. T.; Palstra, T. T. M.; Patenaude, G. W.; Reed, R. W.; Westwood, N. P. C. *J. Am. Chem. Soc.* **1997**, *119*, 2633. [e] Barclay, T. M.; Cordes, A. W.; Haddon, R. C.; Itkis, M. E.; Oakley, R. T.; Reed, R. W.; Zhang, H. *J. Am. Chem. Soc.* **1999**, *121*, 969. [f] Difference in the cathodic peak potentials. [g] Barclay, T. M.; Cordes, A. W.; George, N. A.; Haddon, R. C.; Itkis, M. E.; Mashuta, M. S.; Oakley, R. T.; Patenaude, G. W.; Reed, R. W.; Richardson, J. F.; Zhang, H. *J. Am. Chem. Soc.* **1998**, *120*, 352. [h] Phenalenyl. [i] Not reported.

the number of π electrons. The relaxation energy ΔE^2_{SCF} is related to changes in molecular symmetry upon the reduction to the anion. The largest value is observed for radical **6h** (−15.0 kcal/mol) and smallest for the tricyclic radicals **10** and **11** (about −5 kcal/mol). For comparison, the same calculations for phenalenyl (**12**), an odd-alternant carbocyclic radical originally considered by Haddon,[11] give the lowest values for the two energies: 116.5 kcal/mol for the electron transfer and a negligibly small value of −0.6 kcal/mol for geometry relaxation.

The overall disproportionation energies of the radicals, $\Sigma\Delta E_{SCF}$ and $\Sigma\Delta G_{298}$, decrease with the size of the heterocycle and are lowest for **11** (116.3 kcal/mol and 5.073 eV, respectively). Incidentally, the values calculated for **11** are very close to those for phenalenyl (**12**). The disproportionation energies calculated as $\Sigma\Delta E_0$ (corrected for ZPE) are virtually identical to $\Sigma\Delta E_{SCF}$ and within 0.2 kcal/mol.

Analysis of two pairs of isomers, **6h** and **7h** and **10** and **11**, suggests that the −N−S−S− configuration is more favorable in the disproportionation than is the −S−N−S− sequence of the heteroatoms. For the pair of the two-ring radicals, **6h** and **7h**, the latter has lower energies of the individual and the overall processes by more than 8 kcal/mol. This difference is smaller but is nevertheless still significant (>5 kcal/mol) for the larger three-ring system **10** and **11**.

Results for monocyclic derivatives **1** show that substituents play an important role in modulating the energetics of the disproportionation process. The phenyl substituent in **1g** has the largest effect and lowers the electron transfer and the overall energy by about 15 kcal/mol with respect to the parent **1a**.

Substitution of a nitrogen atom for a CH group lowers the energetics of the individual steps, but the overall energy change $\Sigma\Delta E_{SCF}$ is similar for both heterocycles as apparent from the pair **9h** and **9i** (123.9 and 124.2 kcal/mol, respectively).

A plot of the B3LYP/6-31+G(d)//B3LYP/6-31G(d) calculated energy change $\Sigma\Delta E_{SCF}$ in disproportionation of radicals and the cell electrochemical potential E_{cell} is shown in Figure 6. The plot includes data for radicals exhibiting fully reversible electrochemistry (**1a**, **1g**, **10**, and **11**), and E_{cell} measured for other radicals as a difference in the cathodic peak potentials. The linear regression analysis shows that the correlation for the DFT calculations is poor ($R^2 = 0.69$), reflecting the scattering of the data points in Figure 2. A similar relationship with $R^2 = 0.68$ is obtained using $\Sigma\Delta G_{298}$ for the process.

Solid-state conductivity studied experimentally for four radicals listed in Table 4 qualitatively corresponds to the magnitude of the calculated charge fluctuation energy $\Sigma\Delta E_{SCF}$. The highest conductivity (σ) of about 10^{-4} S/cm at ambient temperature was measured for **11**,[6] which also exhibits the most favorable thermodynamics for the disproportionation. Conversely, radical **1g**, with one of the highest disproportionation energies, is considered to be an insulator ($\sigma < 10^{-9}$ S/cm).

Other Radicals. The established correlations allow for assessment of electron-transfer processes in three known, **3a**, **4c**, and **5**, and two hypothetical radicals, **2a** and **8a**. Data collected in Table 5 show trends similar to those observed for other radicals: the larger the π system, the lower the redox window, the more anodically shifted potentials, and the lower disproportionation energies.

The high electron transfer and relaxation energies ΔE_{SCF} calculated for the monocyclic radicals, **2a** and **3a**, and bicyclic radical **5** seem to preclude them from exhibiting high conductivity. In contrast, **8a** showing $\Sigma\Delta E_{SCF} = 122$ kcal/mol appears to be a reasonable candidate for a molecular semiconductor.

The estimate of oxidation potentials from correlation with I_p uniformly gave unreasonably high values, while potentials obtained from the sum of the calculated cell electrochemical and the reduction potentials, $E^{ox}_{1/2} = E_{cell} + E^{red}_{1/2}$ were close to those expected. Since both correlations $E^{ox}_{1/2}$ (Figure 2) and E_{cell} (Figure 6) are rather poor, it is presumably due to a fortuitous partial cancellation of errors that the latter method works acceptably well, as shown for compounds in Table 5.

TABLE 5: Calculated (B3LYP/6-31+G(d)//B3LYP/6-31G(d)) Parameters for Selected Radicals[a]

	2a	3a	4c	5	8a
$I_{p(vert)}$ [eV][b]	7.47	6.84	8.62[c]	7.55	7.23
EA [eV][d]	1.092	0.662	2.800	1.736	1.840
$E^{red}_{1/2}$ [V][e]	−1.20	−1.53	+0.10	−0.71	−0.44
ΔE^1_{SCF} [kcal/mol]	168.9	162.3	147.7	146.1	129.5
ΔE^2_{SCF} [kcal/mol]	−19.3	−17.2	−16.3	−8.8	−7.4
$\Sigma\Delta E_{SCF}$ [kcal/mol]	149.6	145.1	131.4	137.3	122.1
$\Sigma\Delta G_{298}$ [eV]	6.534	6.332	5.709	5.984	5.614
E_{cell} [V][f]	+1.5	+1.4	+1.25	+1.3	+1.1
$E^{ox}_{1/2}$ [V][g]	+0.3	−0.1	+1.35	+0.6	+0.7

[a] ΔE^1_{SCF} is the electron-transfer energy and ΔE^2_{SCF} is the relaxation energy. $\Sigma\Delta E_{SCF}$ represents the energy of the overall process: $E_{cell} = E^{ox}_{1/2} - E^{red}_{1/2}$. Thermodynamic corrections taken from B3LYP/6−31C(d) calculations. [b] Calculated value scaled by 0.984 (Figure 1a). [c] Experimental value 8.57 eV. See Table 2. [d] Including ZPE correction. [e] Solution reduction potential in acetonitrile calculated from EA (Figure 3). [f] Cell potential calculated from $\Sigma\Delta E_{SCF}$ (Figure 6). [g] Solution oxidation potentials in acetonitrile estimated from the calculated $E^{ox}_{1/2} = E_{cell} + E^{red}_{1/2}$.

For instance, it can be predicted that **4c** has a redox window of 1.25 V in acetonitrile. This value is in good agreement with E_{cell} =1.43 V measured for **4g** in CH_2Cl_2, considering that oxidation potentials in acetonitrile are typically 0.1−0.2 V lower than those in CH_2Cl_2.[8] The predicted ionization potential I_p for **2a** (7.47 eV) is lower than that observed for its isomer **1a** (7.87 eV),[16] which implies a lower oxidation potential for the former. The experimentally observed 0.27 V difference in $E^{ox}_{1/2}$ between **1g** and **2g** suggests that the oxidation potential for **2a** should be about 0.38 V in acetonitrile.[8] The estimate from E_{cell} gives an acceptable value of 0.3 V (Table 5). A reasonably good estimate of $E^{ox}_{1/2}$ is obtained for **3a**, which gives −0.1 V in acetonitrile vs SCE, while the reported oxidation potential measured vs Ag/Ag^+ electrode is near zero V.[29]

The Stability of the −N−S−S− vs −S−N−S− Fragment. The −N−S−S− fragment appears to be generally thermodynamically preferred over −S−N−S−, in which the sulfur atoms terminate the array of heteroatoms. For example, radicals **7h** and **11** are calculated with the B3LYP/6-31G(d) method to be more thermodynamically stable than their −S−N−S− analogs **6h** and **10** by 13.6 and 13.0 kcal/mol, respectively. A similar free energy difference of 15.5 kcal/mol is calculated for the pair of **2d** and **1d**, in which the former readily rearranges to the more stable **1d**.[30]

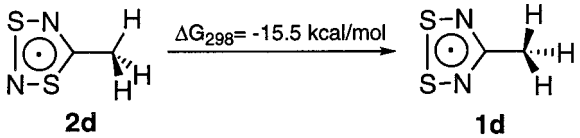

2d **1d**

Summary and Conclusions

In an effort to develop a theoretical tool for designing new molecular materials, we studied gas-phase electron transfer processes for 12 known thioaminyl radicals belonging to 7 general classes of heterocycles using the HF and B3LYP methods with the 6-31G(d) and 6-31+G(d) basis sets. The calculated energy changes were subsequently compared with the experimental I_p and electrochemical redox potentials $E^{ox}_{1/2}$, $E^{red}_{1/2}$, and E_{cell}. Statistical analysis shows that the DFT generally performs better than the HF method, and inclusion of ZPE corrections or thermodynamic parameters in the computed quantities has a negligible effect on the quality of correlations.

The 6-31G(d) basis set was chosen based on favorable comparison of the calculated and experimental normal modes for **1a** and offers a good compromise between accuracy and cost effectiveness. Although the UB3LYP/6-31G(2df) method gave a lower standard deviation for the frequencies (STD = 7 cm^{-1}), the same calculations using the 6-31G(d) basis set gave acceptable results (STD = 11 cm^{-1}). Analogous calculations using the UHF method gave STD almost 3 times larger, indicating low accuracy in computing thermodynamic parameters.

We found that experimental ionization potentials I_p correlate generally well with the B3LYP/6-31G(d) calculated values. Better correlation was obtained for the vertical I_p ($R^2 = 0.993$) than for the adiabatic I_p ($R^2 = 0.969$).

The calculated EA correlates well with the reduction potential of the radicals ($E^{red}_{1/2} = 0.751 \bullet EA - 1.990$, $R^2 = 0.988$, n=10), while the solution oxidation ($E^{ox}_{1/2}$) and the cell electrochemical potentials ($E_{cell} = 0.27 \bullet \Sigma\Delta E_{SCF} - 0.29$, $R^2 = 0.69$, n=10) correlate poorly with the results of gas-phase calculations. Nevertheless, the latter correlation with radical disproportionation energies gives a reasonable estimate for the redox windows E_{cell} of five radicals. Consequently, reasonable oxidation potentials $E^{ox}_{1/2}$ can be obtained from the sum of the estimated potentials $E_{cell} + E^{red}_{1/2}$, while a direct estimate of $E^{ox}_{1/2}$ from the calculated ionization potential I_p gives unrealistically high values.

The calculated disproportionation energies generally decrease with the increasing size of the π system and are smaller for isomers with the −N−S−S− than for the −S−N−S− group. The decrease in disproportionation energy corresponds to the observed increase in conductivity of the radicals. The more favorable behavior of the −N−S−S− isomers has been attributed to higher thermodynamic stability, smaller distortion from planarity upon reduction, lower energies to planarization of the puckered anion, and a higher degree of delocalization.

The correlations established in this work were used to assess properties of five radicals in the context of conductivity of molecular solids. One of them, **8a**, was found to be a good candidate for a molecular semiconductor. Further experimental electrochemical and conductivity studies are needed to establish better correlations and develop theoretical predictive tools. The method can be improved by using higher levels of theory (e.g., basis sets with high angular momentum functions) and larger number of reliable and consistent experimental data. This may provide a quantitative aid in the design of radicals with low energy of charge fluctuation and the general search for molecular conductors.

Acknowledgment. This project was supported by NSF (CHE-9528029) and Vanderbilt University. The author thanks Prof. Larry Schaad for enlightening discussions.

Supporting Information Available: Tables containing calculated SCF energies and thermodynamic parameters for radicals and some ions derived from them. This material is available free of charge via the Internet at http://pubs.acs.org.

References and Notes

(1) Part 1 submitted with this paper: Kaszynski, P. *J. Phys. Chem. A* **2001**, *105*, 7615.

(2) Bryan, C. D.; Cordes, A. W.; Goddard, J. D.; Haddon, R. C.; Hicks, R. G.; MacKinnon, C. D.; Mawhinney, R. C.; Oakley, R. T.; Palstra, T. T. M.; Perel, A. S. *J. Am. Chem. Soc.* **1996**, *118*, 330−338.

(3) Bryan, C. D.; Cordes, A. W.; Fleming, R. M.; George, N. A.; Glarum, S. H.; Haddon, R. C.; MacKinnon, C. D.; Oakley, R. T.; Palstra, T. T. M.; Perel, A. S. *J. Am. Chem. Soc.* **1995**, *117*, 6880−6888.

(4) Cordes, A. W.; Haddon, R. C.; Hicks, R. G.; Kennepohl, D. K.; Oakley, R. T.; Schneemeyer, L. F.; Waszczak, J. V. *Inorg. Chem.* **1993**, *32*, 1554−1558.

(5) Cordes, A. W.; Haddon, R. C.; Oakley, R. T.; Schneemeyer, L. F.; Waszczak, J. V.; Young, K. M.; Zimmerman, N. M. *J. Am. Chem. Soc.* **1991**, *113*, 582−588.

(6) Barclay, T. M.; Cordes, A. W.; Haddon, R. C.; Itkis, M. E.; Oakley, R. T.; Reed, R. W.; Zhang, H. *J. Am. Chem. Soc.* **1999**, *121*, 969−976.

(7) Cordes, A. W.; Haddon, R. C.; Hicks, R. G.; Oakley, R. T.; Vajda, K. E. *Can. J. Chem.* **1998**, *76*, 307−312.

(8) Boeré, R. T.; Roemmele, T. L. *Coord. Chem. Rev.* **2000**, *210*, 369−445.

(9) Boeré, R. T.; Moock, K. H. *J. Am. Chem. Soc.* **1995**, *117*, 4755−4760.

(10) Garito, A. F.; Heeger, A. J. *Acc. Chem. Res.* **1974**, *7*, 232−240.

(11) Haddon, R. C. *Aust. J. Chem.* **1975**, *28*, 2343−51.

(12) Torrance, J. B. *Acc. Chem. Res.* **1979**, *12*, 79−86.

(13) Jursic, B. S. *THEOCHEM*, **1998**, *432*, 211−217.

(14) Boeré, R. T.; Oakley, R. T.; Reed, R. W.; Westwood, N. P. C. *J. Am. Chem. Soc.* **1989**, *111*, 1180−1185.

(15) Cordes, A. W.; Goddard, J. D.; Oakley, R. T.; Westwood, N. P. C. *J. Am. Chem. Soc.* **1989**, *111*, 6147−6154.

(16) Cordes, A. W.; Bryan, C. D.; Davis, W. M.; de Laat, R. H.; Glarum, S. H.; Goddard, J. D.; Haddon, R. C.; Hicks, R. G.; Kennepohl, D. K.; Oakley, R. T.; Scott, S. R.; Westwood, N. P. C. *J. Am. Chem. Soc.* **1993**, *115*, 5, 7232−7239.

(17) Barclay, T. M.; Cordes, A. W.; de Laat, R. H.; Goddard, J. D.; Haddon, R. C.; Jeter, D. Y.; Mawhinney, R. C.; Oakley, R. T.; Palstra, T. T. M.; Patenaude, G. W.; Reed, R. W.; Westwood, N. P. C. *J. Am. Chem. Soc.* **1997**, *119*, 2633−2641.

(18) Patel, M. K.; Huang, J.; Kaszynski, P. *Mol. Cryst. Liq. Cryst.* **1995**, *272*, 87−97.

(19) Kaszynski, P. In *Magnetic Properties of Organic Materials*; P. M. Lahti, Ed.; Marcel Dekker: New York, 1999; pp 305−324.

(20) Farrar, J. M.; Patel, M. K.; Kaszynski, P.; Young, V. G., Jr. *J. Org. Chem.* **2000**, *65*, 931−940.

(21) Benin, V.; Kaszynski, P. *J. Org. Chem.* **2000**, *65*, 8086−8088.

(22) Frisch, M. J.; Trucks, G. W.; Schlegel, H. B.; Gill, P. M. W.; Johnson, B. G.; Robb, M. A.; Cheeseman, J. R.; Keith, T.; Petersson, G. A.; Montgomery, J. A.; Raghavachari, K.; Al-Laham, M. A.; Zakrzewski, V. G.; Ortiz, J. V.; Foresman, J. B.; Cioslowski, J.; Stefanov, B. B.; Nanayakkara, A.; Challacombe, M.; Peng, C. Y.; Ayala, P. Y.; Chen, W.; Wong, M. W.; Andres, J. L.; Replogle, E. S.; Gomperts, R.; Martin, R. L.; Fox, D. J.; Binkley, J. S.; Defrees, D. J.; Baker, J.; Stewart, J. P.; Head-Gordon, M.; Gonzalez, C.; Pople, J. A. *Gaussian 94*, revision E.1; Gaussian, Inc.: Pittsburgh, PA, 1995.

(23) Frisch, M. J.; Trucks, G. W.; Schlegel, H. B.; Scuseria, G. E.; Robb, M. A.; Cheeseman, J. R.; Zakrzewski, V. G.; Montgomery, J. A., Jr.; Stratmann, R. E.; Burant, J. C.; Dapprich, S.; Millam, J. M.; Daniels, A. D.; Kudin, K. N.; Strain, M. C.; Farkas, O.; Tomasi, J.; Barone, V.; Cossi, M.; Cammi, R.; Mennucci, B.; Pomelli, C.; Adamo, C.; Clifford, S.; Ochterski, J.; Petersson, G. A.; Ayala, P. Y.; Cui, Q.; Morokuma, K.; Malick, D. K.; Rabuck, A. D.; Raghavachari, K.; Foresman, J. B.; Cioslowski, J.; Ortiz, J. V.; Stefanov, B. B.; Liu, G.; Liashenko, A.; Piskorz, P.; Komaromi, I.; Gomperts, R.; Martin, R. L.; Fox, D. J.; Keith, T.; Al-Laham, M. A.; Peng, C. Y.; Nanayakkara, A.; Gonzalez, C.; Challacombe, M.; Gill, P. M. W.; Johnson, B. G.; Chen, W.; Wong, M. W.; Andres, J. L.; Head-Gordon, M.; Replogle, E. S.; Pople, J. A. *Gaussian 98*, revision A.7; Gaussian, Inc.: Pittsburgh, PA, 1998.

(24) Clark, T.; Chandrasekhar, J.; Spitznagel, G. W.; Schleyer, P. v. R. *J. Comput. Chem.* **1983**, *4*, 294−301.

(25) Scott, A. P.; Radom, L. *J. Phys. Chem.* **1996**, *100*, 16502−16513.

(26) Barclay, T. M.; Cordes, A. W.; George, N. A.; Haddon, R. C.; Itkis, M. E.; Mashuta, M. S.; Oakley, R. T.; Patenaude, G. W.; Reed, R. W.; Richardson, J. F.; Zhang, H. *J. Am. Chem. Soc.* **1998**, *120*, 352−360.

(27) Sandman, D. J.; Ceasar, G. P. *Isr. J. Chem.* **1986**, *27*, 293−299.

(28) Boeré, R. T.; Moock, K. H.; Parvez, M. *Z. Anorg. Allg. Chem.* **1994**, *620*, 1589−1598.

(29) MacLean, G. K.; Passmore, J.; Rao, M. N. S.; Schriver, M. J.; White, P. S.; Bethell, D.; Pilkington, R. S.; Sutcliffe, L. H. *J. Chem. Soc., Dalton Trans.* **1985**, 1405−1416.

(30) Burford, N.; Passmore, J.; Schriver, M. J. *J. Chem. Soc., Chem. Commun.* **1986**, 140−142.